Instabilities of Flows over Bodies at Large Incidence

David Degani*
NASA Ames Research Center, Moffett Field, California 94035

The phenomena of the flow about an ogive-cylinder placed at incidence to an oncoming stream were numerically investigated for angles of attack of 60 and 80 deg. It was found that the flow around the cylindrical part of the body became unsteady, and vortex shedding was observed. For the 80-deg case, the corresponding Strouhal frequency was about 0.2, which is in agreement with the average value of the Strouhal frequency for flow around a two-dimensional cylinder. For both angles of attack, a small temporal disturbance of finite duration was sufficient to trigger the unsteadiness, which evolved to a finite amplitude fluctuation in the wake. Therefore, it seems possible that the origin of flow unsteadiness and vortex shedding in the wake is an absolute-type instability of the originally steady flow. When a permanent disturbance was also added near the tip of the body in the case of 60-deg angle of attack, a pair of steady, asymmetric vortices emerged from the vicinity of the body nose. These vortices could be the result of a convective-type instability of the originally symmetric flow. It appears that both types of instability may coexist.

Nomenclature

a_∞ = speed of sound
C_N = normal-force coefficient
C_p = pressure coefficient
C_Y = side-force coefficient
D = maximum diameter of body
h = disturbance height
M_∞ = freestream Mach number
Re_D = Reynolds number based on D
$\tilde{t}$ = nondimensional time, ta_∞/D
x,y,z = coordinate system
α = angle of attack
ξ,η,ζ = computational coordinate system
ρ = density
ϕ = circumferential roll angle

Introduction

THE mechanisms that lead to an asymmetric vortex wake in three-dimensional flow over a body of revolution at incidence are not well understood at the present time.[1,2] Several mechanisms for laminar and fully turbulent flows[3,4] and for transitional flows[5] have been advanced but none of them has been found to be satisfactory.

At a low angle of attack, the flow, as observed experimentally,[4,6-10] is almost symmetric. Results of previous thin-layer Navier-Stokes computations[11-14] for vortical flow over an ogive-cylinder body at $\alpha = 20$ deg were perfectly symmetric and agreed very well with experimental measurements.[4] Introducing a small geometric perturbation[15] near the tip of the body had only small effect on the flowfield. The vortical flowfield above the body had very little asymmetry and the primary vortices were almost parallel and located close to the upper body surface.

Presented in part as Paper 90-0593 at the AIAA 28th Aerospace Sciences Meeting, Reno, NV, Jan. 8-11, 1990; received May 7, 1990; revision received Jan. 25, 1991; accepted for publication Jan. 25, 1991.

*NRC Senior Research Associate; Associate Professor, Faculty of Mechanical Engineering, on leave from Technion-Israel Institute of Technology, Haifa 3200, Israel. Associate Fellow AIAA.

It was found experimentally (cf., Refs. 4,6-10,16) that at an angle of attack of 40 deg, as the size or the location of the disturbance changed, for example, the roll-angle position of a small geometric bump near the tip of the nose, the position of the first pair of primary vortices changed in a continuous way. Sometimes, the variation with roll-angle position of the nose became almost periodic,[10] where at the crossover points the vortices became almost symmetric. It was also observed that, for a given configuration, there was a maximum extent of vortex asymmetry such that an increase in the level of the disturbance did not further increase the extent of asymmetry.[16]

Previous Navier-Stokes computations[11-13] showed that even for an angle of attack of 40 deg the computed flow remained symmetric and was stable to small, temporal perturbations. When a space-fixed, time-invariant perturbation was introduced into the computation, the flowfield became highly asymmetric.[13,15] The flow asymmetry in the vicinity of the disturbance was very small but grew rapidly beyond the point where the primary vortices curve away from the body. When the disturbance (a small jet in Ref. 13) was removed, the flowfield relaxed back to a symmetric state.[11-13] On the other hand, when a geometric perturbation was used and its height was cut to one half of the original size (from 1.0 to 0.5% of the body diameter), the computational results show a small decrease in the extent of asymmetry but a change in sign of the total side-force coefficient.

On the basis of the observed character of the flow, namely, the rapid growth of the disturbances in the wake of the body, and the fact that upon removal of the disturbance the wake relaxed back to the original symmetric flowfield, it was suggested[15] that the asymmetric flow that exists at $\alpha = 40$ deg is the result of disturbing a convectively unstable symmetric flow. The basis for the suggestion becomes clear when it is recalled that, for a convectively unstable flow, initially growing disturbances that are triggered by a short-duration excitation will be washed downstream and, in the absence of further excitation, the flow will return to its original undisturbed state.

The situation changed when the angle of attack was increased above 50 deg. Experiments[10] showed that the variation of the side force with nose roll angle changed from a continuous distribution to one approaching a square wave, and the amplitude of the side force decreased as the angle of attack increased. For angles of attack >60 deg, the flowfield exhibited a significant amount of unsteadiness due to periodic vortex shedding in the wake behind the cylindrical portion of

the body, and the mean side-force variation with nose angle was almost zero.

In the current work, computations based on a thin-layer Navier-Stokes code have been applied to further investigate the phenomena governing the onset of vortex asymmetry and vortex shedding at these high angles of attack. Time-accurate solutions were obtained for flow over an ogive-cylinder body for angles of attack of $\alpha = 60$ and 80 deg and a Reynolds number (based on freestream conditions and cylinder diameter) $Re_D = 2 \times 10^5$.

Theoretical Background

The dimensionless conservation equations of mass, momentum, and energy can be represented in a flux-vector form that is convenient for numerical simulation as[17]

$$\partial_\tau \hat{Q} + \partial_\xi(\hat{F} + \hat{F}_v) + \partial_\eta(\hat{G} + \hat{G}_v) + \partial_\zeta(\hat{H} + \hat{H}_v) = 0 \quad (1)$$

where τ is the time and the independent spatial variables ξ, η, and ζ are chosen to map a curvilinear body-conforming grid into a uniform computational space. In Eq. (1), $\hat{Q}$ is the vector of dependent flow variables; $\hat{F} = \hat{F}(\hat{Q})$, $\hat{G} = \hat{G}(\hat{Q})$, and $\hat{H} = \hat{H}(\hat{Q})$ are the inviscid flux vectors, and the terms $\hat{F}_v$, $\hat{G}_v$, and $\hat{H}_v$ are fluxes containing the viscous derivatives.

For body-conforming coordinates and high Reynolds number flow, if ζ is the coordinate leading away from the surface, the thin-layer approximation can be applied, which yields[18,19]

$$\partial_\tau \hat{Q} + \partial_\xi \hat{F} + \partial_\eta \hat{G} + \partial_\zeta \hat{H} = Re^{-1}\partial_\zeta \hat{S} \quad (2)$$

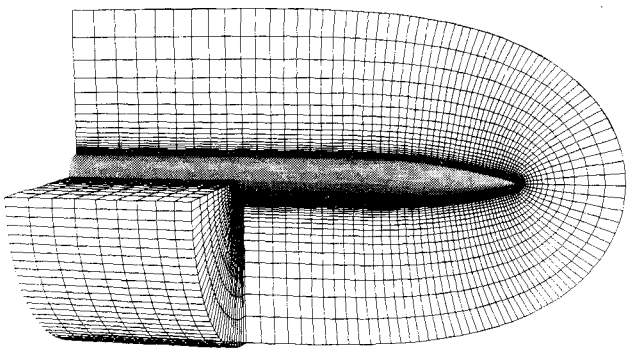

Fig. 1 Tangent ogive-cylinder grid.

where only viscous terms in ζ are retained. These have been collected into the vector $\hat{S}$, and the nondimensional Reynolds number Re is factored from the viscous flux term.

The implicit scheme employed in this study is the algorithm reported by Steger et al.[20] The algorithm uses flux-vector splitting[21] and upwind spatial differencing for the convection terms in one coordinate direction (nominally streamwise). As discussed in Ref. 20, schemes using upwind differencing can have several advantages over methods that utilize central spatial differences in each direction. In particular, such schemes can have natural numerical dissipation and better stability properties. By using upwind differencing for the convective terms in the streamwise direction while retaining central differencing in the other directions, a two-factor implicit approximately factored algorithm is obtained. Additional details of the numerical algorithm can be found in Ref. 20.

Computations were performed for subsonic flow over an ogive-cylinder body, which consisted of a 3.5-diam tangent ogive forebody with a 7.0-diam cylindrical afterbody extending aft of the nose-body junction to $x/D = 10.5$. The grid consisted of 120 equispaced circumferential planes ($\Delta\phi = 3$ deg) extending completely around the body. In each circumferential plane, the grid contained 50 radial points between the body surface and the computational outer boundary and 59 axial points between the nose and the rear of the body (Fig. 1). This grid spacing was found adequate for similar flowfields in previous calculations.[11-13]

An adiabatic no-slip boundary condition was applied at the body surface, whereas undisturbed freestream conditions were maintained at the computational outer boundary. An implicit periodic continuation condition was imposed at the circumferential edges of the grid, whereas at the downstream boundary, a simple zero-axial-gradient extrapolation condition was applied. This simple extrapolation boundary condition is not strictly valid in subsonic flow since the body wake can affect the flow on the body. However, by letting both computed body lengths extend beyond the physical length of the experimental model[6,7] and by neglecting the portion of the flow near the downstream boundary, the effect of the boundary can be minimized. On the upstream axis of symmetry, an extrapolation boundary condition was used to obtain the flow conditions on the axis from the cone of points one axial plane downstream.

In these computations, a time-accurate solution was required. Thus, the second-order time-accurate algorithm was used with a globally constant time step. The flowfield was

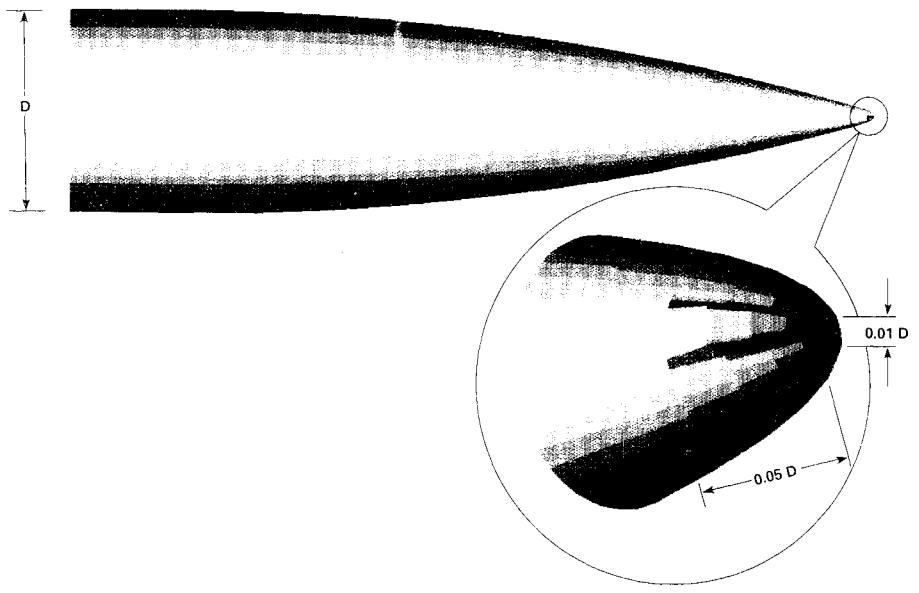

Fig. 2 Geometrical disturbance.

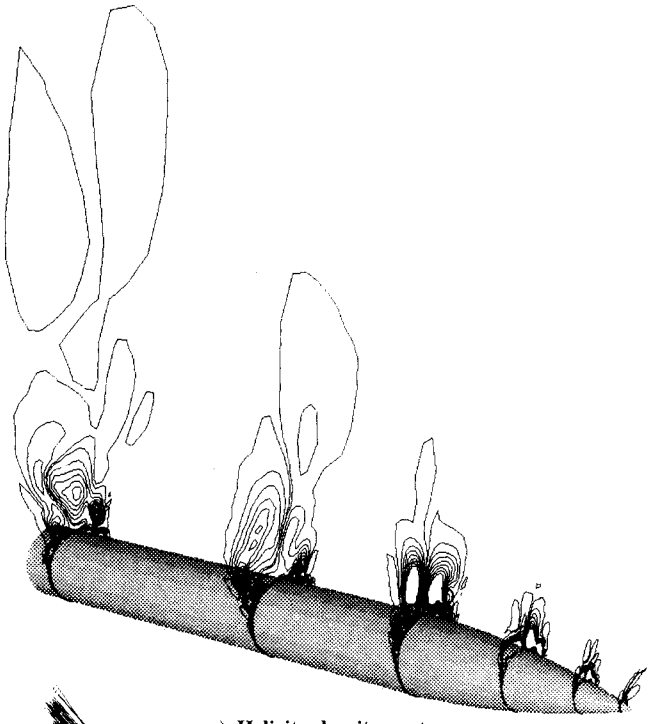

a) Helicity density contours

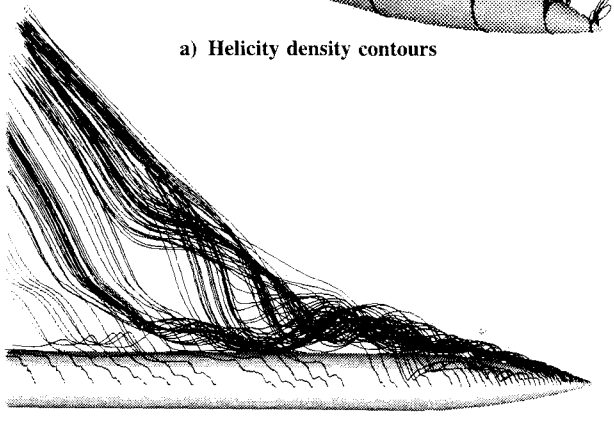

b) Off-surface streamlines

Fig. 3 Computational results (without geometrical disturbance) for α = 60 deg, M_∞ = 0.2, and $Re_D = 2 \times 10^5$.

initially set to freestream conditions throughout the grid, or to a previously obtained solution, and the flowfield was advanced in time until a solution was obtained.

A small geometric bump was added to the body surface to act as a symmetry-breaking perturbation (Fig. 2). The height of the bump ranged from 0.005 to 0.02 of the body cylinder diameter, the length of the bump was 0.05 of the body diameter, and it was located at $x/D \approx 0.025$ and 90 deg circumferentially from the windward meridian.

The code required approximately 8×10^{-5} s/iteration/grid point on the NAS CRAY-2 computer. This translates to approximately 27 s/iteration. Further, the need to resolve the thin viscous layers for high Reynolds number flow required that the grid have a fine radial spacing at the body surface. As a result, the allowable computational nondimensional time steps were found to range from 0.008 to 0.010.

Results

α = 60 Degrees

Experiments[6,7,10] showed that at angles of attack larger than 50 deg the flowfield exhibited a significant amount of unsteadiness due to vortex shedding in the wake of the flow over the cylindrical portion of the body. Vortex shedding from a two-dimensional cylinder can be described as a phenomenon involving absolute instability, which means that, in order to

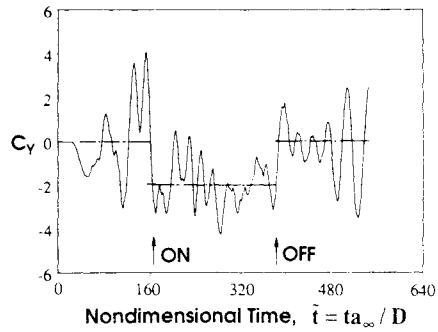

Fig. 4 Side-force coefficient history: α = 60 deg; M_∞ = 0.2; $Re_D = 2 \times 10^5$.

move the flowfield from an unstable symmetric wake to a self-sustained oscillation of the wake, it is sufficient to introduce a symmetry-breaking perturbation only for a short period of time. It remains to be seen whether the origin of unsteadiness and vortex shedding for a finite-length body also can be described as an absolute instability of an originally steady symmetric flow.

To test this computationally, a case was initiated for α = 60 deg, with the initial solution that of the symmetric α = 40-deg case. A small change of flow density was imposed in a small volume on one side of the body near the tip. The perturbation was removed after the total side force (which was zero at the beginning of the process) became about 5% of the total normal force (at $\tilde{t}$ = 32, Fig. 4). The flowfield continued to evolve to an unsteady oscillating one. The flow is instantaneously highly asymmetric even without the presence of a permanent geometric disturbance, but is fluctuating around a symmetric mean. From Figs. 3, which show the helicity density[22,23] contours and the corresponding off-surface instantaneous streamlines, the fact that the flowfield is highly asymmetric becomes more evident. The first pair of primary vortices does not curve away from the nose as one would expect, but rather stays parallel to the body upper surface and ultimately curve away only on the aft part of the body. It is also evident that all four vortices interact with each other in a relatively small space above the aft part of the body. As a result, the instantaneous streamlines do not form tight vortices but are diffuse. It was also found that all vortices change their positions as time evolves, moving back and forth with a small amplitude, possibly correlated with the changes in the side force.

From experimental observations[6,7,16] for an angle of attack of α = 60 deg, it was expected that the first pair of vortices would lift off near the tip. This behavior was not observed in the computational results. Based on the flow behavior observed at α = 40 deg, it seemed plausible that, in order to excite the tip vortices, a space-fixed, time-invariant perturbation would again be needed. Accordingly, another computational experiment was conducted by adding a geometric disturbance (h/D = 0.01) at $x/D \approx 0.025$ on the nose of the body. The computations were continued using the previous solution as an initial solution. Figure 4 presents the time history of the side-force coefficients. Up to the time when the permanent perturbation was added (marked by the "ON" arrow), the flow was unsteady but fluctuated around a symmetric mean flow. After the geometric disturbance was added, the flow still exhibited large-amplitude oscillations in side force, but the fluctuating flow developed an asymmetric mean component. This is also evident from the helicity density contours and the corresponding off-surface instantaneous streamlines (Figs. 5). Immediately after the geometric disturbance was added, a relatively weak vortex lifted off near the tip on the side of the nose where the disturbance was located. Later, after a development that took $\Delta\tilde{t}$ = 25 (which is about the time for a particle in the flow to travel three body lengths), a second, stronger vortex lifted off from the opposite side of

the nose. At the same time, the vortices above the cylindrical afterbody continued to be unsteady, analogous to the unsteadiness that existed before the disturbance was introduced on the nose. Again, the instantaneous streamlines above the aft cylindrical portion of the body do not form tight vortices; they fill the whole space between the body and the second primary vortex, and they move back and forth with time, similar to experimental observations (cf. Fig. 6, taken from Ref. 10). Finally, when the disturbance was removed (marked by the "OFF" arrow in Fig. 4), the flow returned to oscillate around a symmetric mean with about the same frequency as before. These computational results are also consistent with recent experimental observations.[24]

α = 80 Degrees

For technical reasons, the cylindrical portion of the body for the case of α = 80 deg is shorter (L/D = 6.5) than that used for the other cases. From experiment,[6,7,10] it is known that at this angle of attack the flow about the cylindrical portion of the body should be fluctuating at a Strouhal number of about 0.21 (the Strouhal number of flow around a two-dimensional cylinder under the same flow conditions). The computations were started from uniform freestream flow. A short time perturbation, similar to the one used for the α = 60-deg case, was imposed. The flowfield very rapidly became oscillatory, with fluctuations yielding highly asymmetric instantaneous flows around a symmetric mean. Figure 7 shows the time history of the side-force coefficient for this case. It is obvious that vortices are being shed but in an irregular manner. This is due in part to the relatively short time since the flow was started from rest, to the high Reynolds number of the laminar flow, to high-frequency riders, and to three-dimensional effects of the short body. Nevertheless, Fourier analysis of the time history shows that, aside from the high-frequency riders, the equivalent Strouhal number for the dominant frequency is about 0.2. Figures 8 show four successive snapshots of helicity density contours in cross sections of the flowfield above the body. These snapshots represent about one cycle of the low-frequency oscillation. In the rearmost cross section of each snapshot, each vortex is marked with + or − to indicate the direction of the rotation of the vortex.

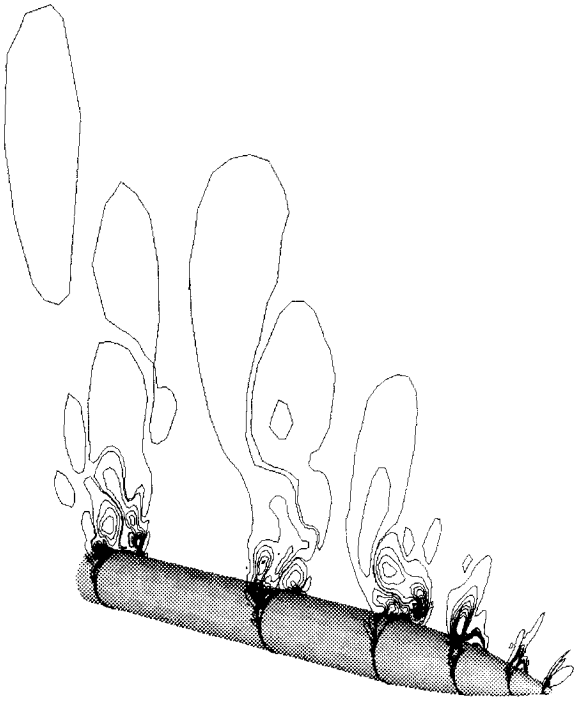

a) Helicity density contours

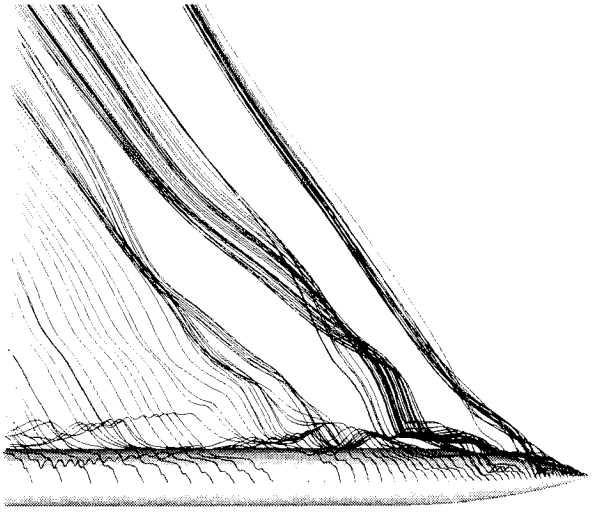

b) Off-surface streamlines

Fig. 5 Computational results (with geometrical disturbance) for h/D = 0.01, α = 60 deg, M_∞ = 0.2, and Re_D = 2 × 10^5.

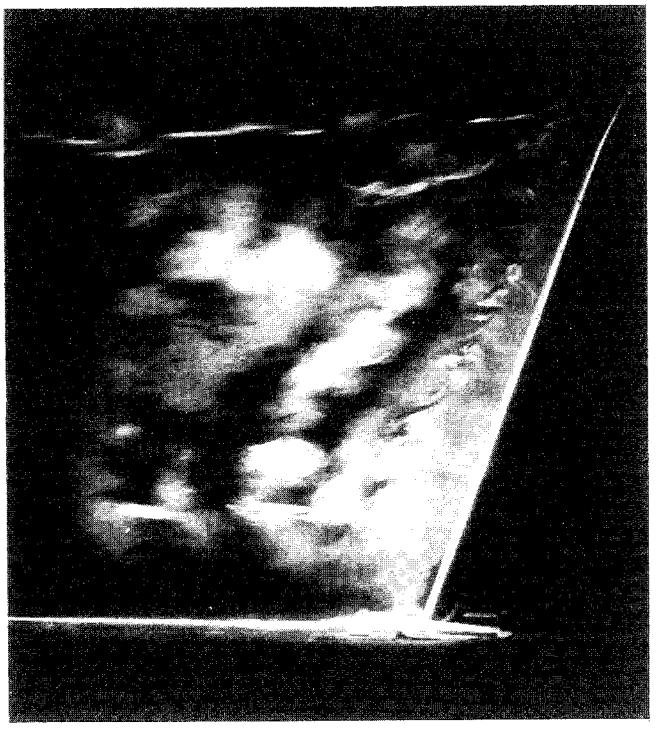

Fig. 6 Smoke-laser-sheet visualization of the wake behind an ogive cylinder: α = 70 deg; Re_D = 3 × 10^4 (from Ref. 10).

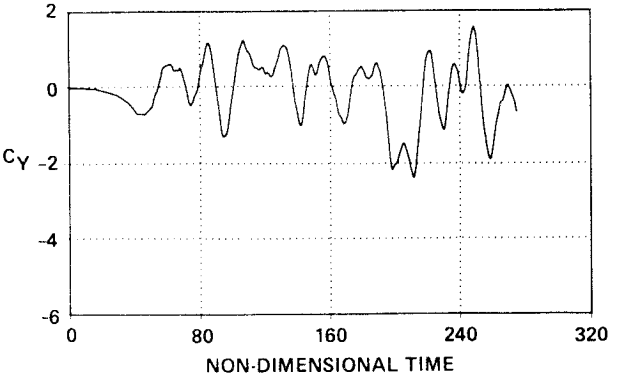

Fig. 7 Side-force coefficient history: α = 80 deg; M_∞ = 0.2; Re_D = 2 × 10^5.

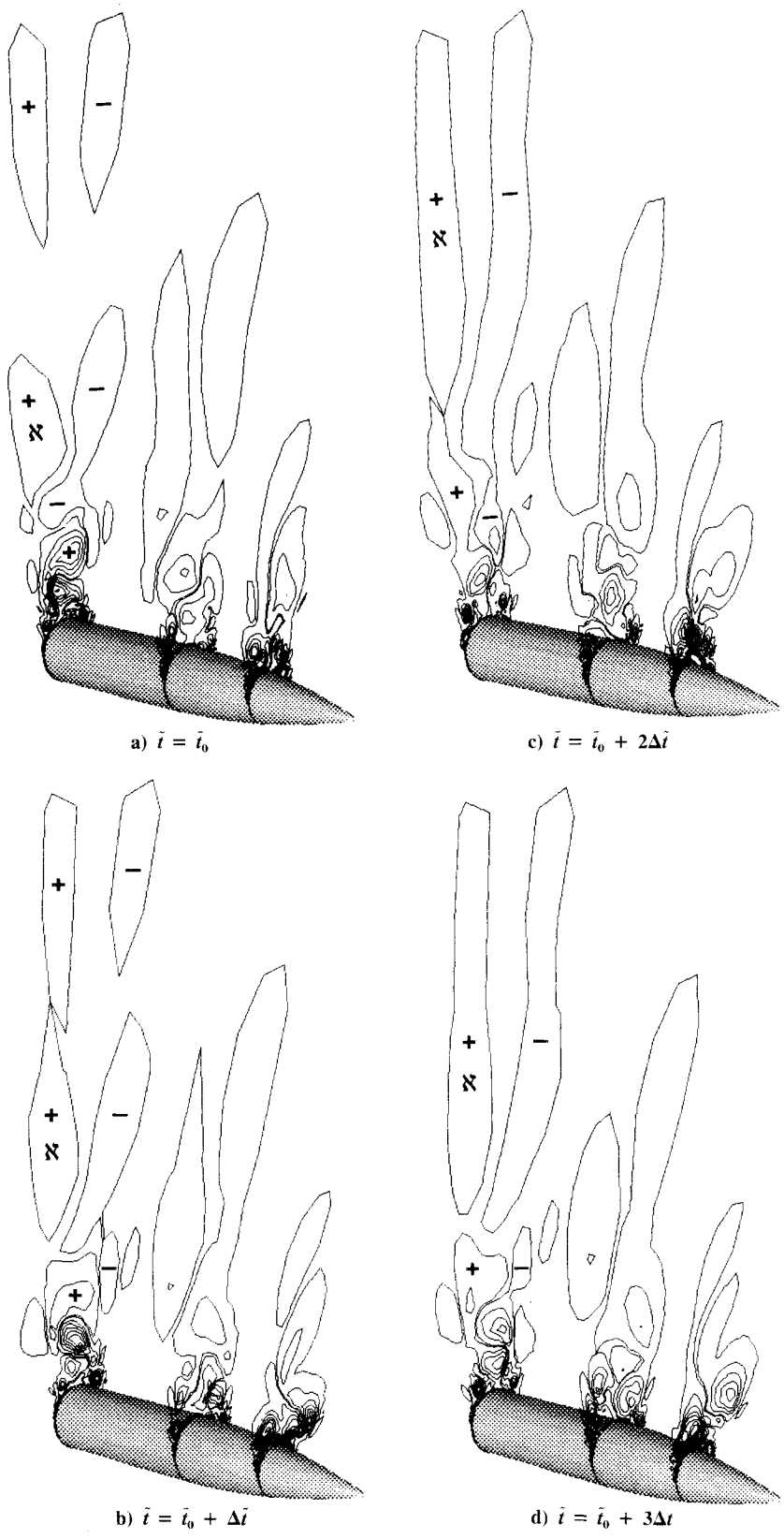

Fig. 8 Helicity density contours: $\alpha = 80$ deg; $M_\infty = 0.2$; $Re_D = 2 \times 10^5$.

By following one vortex as it develops with time (for example, the one which is marked ℵ in Fig. 8a), it is clear that the vortex moves upward as time progresses and a new vortex starts to develop underneath it. Figures 9 show a close-up view of the rearmost cross section of each snapshot of Figs. 8 in the area near the cylinder surface. The unsteadiness of the shear layer can be seen clearly. Small-scale vortices are formed and move along the shear layer, finally merging with the primary vortex. A small vortex is formed in the shear layer (marked as 1), moves upward, and merges into the primary vortex above it. Meanwhile, a new vortex is forming below it (marked 2 in Fig. 9d). This unsteadiness is probably responsible for the high-frequency component observed in the time history of the side force.

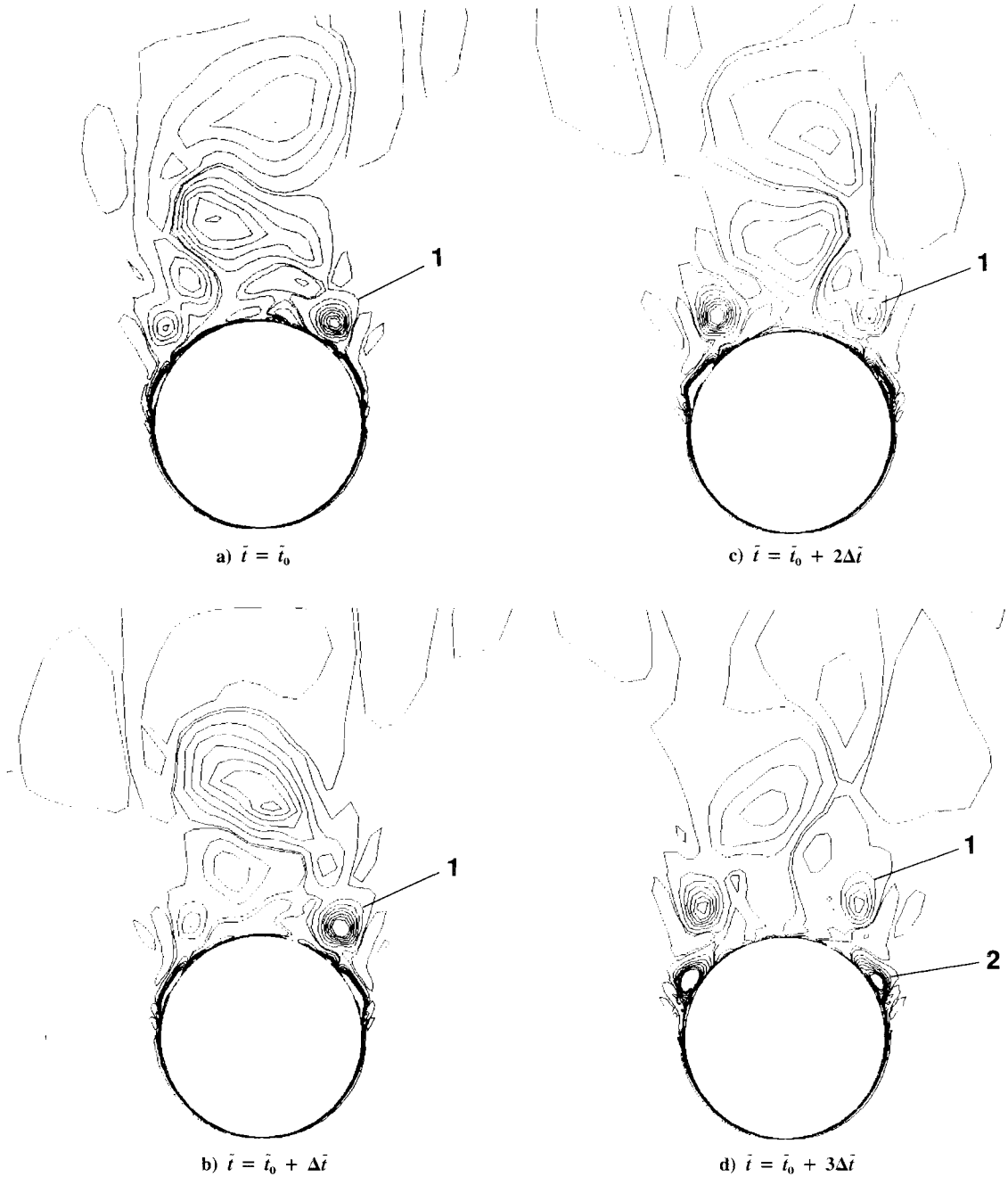

Fig. 9 Helicity density contours: $x/D = 6.0$; $\alpha = 80$ deg; $M_\infty = 0.2$; $Re_D = 2 \times 10^5$.

Discussion and Conclusions

As mentioned earlier, the unsteady Karman vortex shedding that develops downstream of a two-dimensional cylinder in crossflow (at $Re_D \geq 50$) is the result of an absolute instability[25-27] of the originally symmetric flow. This means that, in the absence of any perturbation, the flow would remain symmetric and that any initial disturbance will grow in time and space. Because of nonlinear effects, the growth of the disturbance will reach an equilibrium state and the flow will evolve to a self-sustained oscillation of the wake. Indeed, time-accurate computations of two-dimensional flow about a circular cylinder[28-30] (using algorithms that are unbiased in the circumferential direction) have revealed that, unless a symmetry-breaking perturbation was introduced into the flow, the solutions remained symmetric and steady. The perturbations were typically introduced for a short period of time, then removed, and the flows advanced in time until the oscillatory solution was developed.

In the case of flow around the three-dimensional ogive-cylinder body, as the angle of attack approaches $\alpha = 90$ deg, the flow behavior in the wake of the cylindrical part of the body is similar to the Karman vortex shedding behind a two-dimensional cylinder. Experiments[6,7] showed that, even for angles of attack as low as $\alpha = 60$ deg, vortices are shed in the wake of the cylindrical part of the body. The Strouhal number varies with $\sin(\alpha)$, approaching the classical two-dimensional cylinder value as the angle of attack approaches $\alpha = 90$ deg. This is also indicated by the numerical calculations presented here for the $\alpha = 80$-deg case. The calculations also show that even for $\alpha = 60$ deg there was vortex shedding in the wake of the cylindrical part of the body. For both angles of attack ($\alpha = 60$ and 80 deg), a small temporal disturbance of finite duration was sufficient to trigger the unsteadiness that evolved to a finite-amplitude fluctuation in the wake. These observations are consistent with the notion of absolute-type instability (of the originally steady flow). On the other

hand, in order to obtain the experimentally observed pair of asymmetric, steady tip vortices, a space-fixed, permanent disturbance was required in the computations. The latter may represent a convective instability[26,31-33] of the symmetric flow. The results also indicate the possibility that, for certain angles of attack, the flow around pointed, slender bodies may contain both instability mechanisms. The coexistence of the two instability mechanisms was also deduced by Yang and Zebib[26] from their computations for the unsteady wake behind a two-dimensional cylinder.

Acknowledgment

The author wishes to thank Murray Tobak and Lewis Schiff for helpful discussions.

References

[1]Hunt, B. L., "Asymmetric Vortex Forces and Wakes on Slender Bodies," AIAA Paper 82-1336, Aug. 1982.

[2]Ericsson, L. E., and Reding, J. P., "Aerodynamic Effects of Asymmetric Vortex Shedding from Slender Bodies," AIAA Paper 85-1797, Aug. 1985.

[3]Tobak, M., Chapman, G. T., and Unal, A., "Modeling Aerodynamic Discontinuities and Onset of Chaos in Flight Dynamical Systems," *Annale des Telecommunications*, Vol. 42, No. 5-6, 1987.

[4]Lamont, P. J., "Pressures Around an Inclined Ogive-Cylinder with Laminar, Transitional, or Turbulent Separation," *AIAA Journal*, Vol. 20, No. 11, 1982, pp. 1492-1499.

[5]Keener, E. R., and Chapman, G. T., "Similarity in Vortex Asymmetries over Slender Bodies and Wings," *AIAA Journal*, Vol. 15, No. 9, 1977, pp. 1370-1372.

[6]Degani, D., and Zilliac, G. G., "Experimental Study of Unsteadiness of the Flow Around as Ogive-Cylinder at Incidence," AIAA Paper 88-4330, Aug. 1988.

[7]Degani, D., and Zilliac, G. G., "An Experimental Study of the Nonsteady Asymmetric Flow Around an Ogive-Cylinder at Incidence," *AIAA Journal*, Vol. 28, No. 4, 1990, pp. 642-649.

[8]Hunt, B. L., and Dexter, P. C., "Pressures on a Slender Body at High Angle of Attack in a Very Low Turbulence Level Airstream," *High Angle of Attack Aerodynamics*, AGARD-CP-247, Paper 17, 1978.

[9]Dexter, P. C., and Hunt, B. L., "The Effects of Roll Angle on the Flow over a Slender Body of Revolution at High Angle of Attack," AIAA Paper 81-0358, Jan. 1981.

[10]Zilliac, G. G., Degani, D., and M. Tobak, "Asymmetric Vortices on a Slender Body of Revolution," AIAA Paper 90-0388, Jan. 1990.

[11]Degani, D., and Schiff, L. B., "Numerical Simulation of Asymmetric Vortex Flows Occurring on Bodies of Revolution at Large Incidence," AIAA Paper 87-2628, Aug. 1987.

[12]Degani, D., and Schiff, L. B., "Numerical Simulation of the Effect of Spatial Disturbances on Vortex Asymmetry," AIAA Paper 89-0340, Jan. 1989.

[13]Degani, D., and Schiff, L. B., "Numerical Simulation of the Effect of Spatial Disturbances on Vortex Asymmetry," *AIAA Journal*, Vol. 29, No. 3, 1991, pp. 344-352.

[14]Schiff, L. B., Degani, D., and Gavali, S,. ' Numerical Simulation of Vortex Unsteadiness on Slender Bodies of Revolution at Large Incidence," AIAA Paper 89-0195, Jan. 1989.

[15]Degani, D., "Numerical Study of the Effect of Geometrical Disturbances on Vortex Asymmetry," *AIAA Journal*, Vol. 29, No. 4, 1991, pp. 560-566.

[16]Moskovitz, C. A., Hall, R. M., and DeJarnette, F. R., "Effects of Nose Bluntness, Roughness and Surface Perturbations on the Asymmetric Flow Past Slender Bodies at Large Angles of Attack," AIAA Paper 89-2236, Aug. 1989.

[17]Viviand, H., "Conservative Forms of Gas Dynamics Equations," *La Recherche Aerospatiale*, No. 1, Jan.-Feb. 1974, pp. 65-68.

[18]Baldwin, B. S., and Lomax, H., "Thin Layer Approximation and Algebraic Model for Separated Turbulent Flows," AIAA Paper 78-257, Jan. 1978.

[19]Steger, J. L., "Implicit Finite-Difference Simulation of Flow About Arbitrary Two-Dimensional Geometries," *AIAA Journal*, Vol. 16, No. 7, 1978, pp. 679-686.

[20]Steger, J. L., Ying, S. X., and Schiff, L. B., "A Partially Flux-Split Algorithm for Numerical Simulation of Compressible Inviscid and Viscous Flows," *Proceedings: Workshop on Computational Fluid Dynamics*, Univ. of California, Davis, CA, 1986.

[21]Steger, J. L., and Warming, R. F., "Flux Vector Splitting of the Inviscid Gasdynamic Equations with Applications to Finite-Difference Methods," *Journal of Computational Physics*, Vol. 40, No. 2, 1981, pp. 263-293.

[22]Levy, Y., Seginer, A., and Degani, D., "Graphical Representation of Three-Dimensional Vortical Flows by Means of Helicity Density and Normalized Helicity," AIAA Paper 88-2598, June 1988.

[23]Levy, Y., Degani, D., and Seginer, A., "Graphical Visualization of Three-Dimensional Vortical Flows by Means of Helicity," *AIAA Journal*, Vol. 28, No. 8, 1990, pp. 1347-1352.

[24]Degani, D., and Tobak, M., "Numerical, Experimental and Theoretical Study of Convective Instability of Flows over Pointed Bodies at Incidence," AIAA Paper 91-0291, Jan. 1991.

[25]Triantafyllou, G. S., Kupfer, K., and Bers, A., "Absolute Instabilities and Self-Sustained Oscillation in the Wakes of Circular Cylinder," *Physical Review Letters*, Vol. 59, 1987, pp. 1014-1917.

[26]Yang, X., and Zebib, A., "Absolute and Convective Instability of a Cylinder Wake," *Physics of Fluids*, Vol. 4, 1989, pp. 689-696.

[27]Chomaz, J. M., Huerre, P., and Redekopp, L. G., "Bifurcations to Local and Global Modes in Spatially Developing Flows," *Physical Review Letters*, Vol. 60, 1988, pp. 25-28.

[28]Patel, V. A., "Karman Vortex Street Behind a Circular Cylinder by the Series Truncation Method," *Journal of Computational Physics*, Vol. 28, 1978, pp. 14-42.

[29]Lecointe, Y., and Piquet, J., "On the Use of Several Compact Methods for the Study of Unsteady Incompressible Viscous Flow Round a Circular Cylinder," *Computers & Fluids*, Vol. 12, No. 4, 1984, pp. 255-280.

[30]Rosenfeld, M., Kwak, D., and Vinokur, M., "A Solution Method for the Unsteady and Incompressible Navier-Stokes Equations in Generalized Coordinate Systems," AIAA Paper 88-0178, Jan. 1988.

[31]Wilkinson, S. P., and Malik, M. R., "Stability Experiments in the Flow over a Rotating Disk," *AIAA Journal*, Vol. 23, No. 4, 1985, pp. 588-595.

[32]Gaster, M., "The Role of Spatially Growing Waves in the Theory of Hydrodynamic Stability," *Progress in Aeronautical Sciences*, Vol. 6, edited by D. Kuchemann and L. H. G. Sterne, Pergamon, Oxford, England, UK, 1965.

[33]Schubauer, G. B., and Skramstad, H. K., "Laminar Boundary Layer Oscillations and Transition on a Flat Plate," NACA Rept. 909, 1949.